

SUBSTRATE CHARACTERISTICS OF $\text{Ba}_2\text{HoNbO}_6$ FOR THE FABRICATION OF $\text{LaBaCaCu}_3\text{O}_{7-\delta}$ SUPERCONDUCTING FILMS

D. A. LANDÍNEZ TÉLLEZ*, J. ALBINO AGUIAR†, Y. P. YADAVA†, E. CHAVIRA‡
and J. ROA-ROJAS*,§

* *Departamento de Física, Universidad Nacional de Colombia,
A.A. 14490, Bogotá DC, Colombia*

§ *jroa@multi.net.co*

† *Departamento de Física, Universidade Federal de Pernambuco,
50970-901, Recife, PE, Brazil*

‡ *Instituto de Investigaciones en Materiales, Universidad Autónoma de México,
A.P. 70630, 04510 México-DF, México*

Received 22 August 2001

We have synthesized and studied the characteristics of $\text{Ba}_2\text{HoNbO}_6$ (BHNO) substrates for the fabrication of $\text{LaBaCaCu}_3\text{O}_{7-\delta}$ (LBCCO) superconducting films. BHNO has an $\text{A}_2\text{BB}'\text{O}_6$ complex cubic perovskite structure with lattice constant $a = 8,439 \text{ \AA}$. Energy-dispersive X-ray (EDX) analysis shows that BHNO is free from impurity traces and scanning electron micrographs reveal that it has uniform surface morphology and particle size distribution. Based on the doubling of the ABO_3 cubic perovskite unit cell, $(1/2)a = 4,220 \text{ \AA}$, BHNO has fairly good lattice matching (lattice mismatch $\sim 9\%$) with LBCCO superconductors. X-ray diffractometry, back-scattered scanning electron microscopy and magnetic measurements effectuated on BHNO/LBCCO composites show that BHNO is chemically and physically compatible and it could be used as a potential substrate material for the growth of LBCCO superconducting films.

PACS Number(s): 74.72.-h, 74.25.-q, 61.66.-f, 61.10.-i

1. Introduction

At present, the investigation on new substrate materials for high temperature superconducting films is a significant concern in materials research for their use in various electronic device applications. In recent years, complex perovskite oxides have been investigated for their use as potential new substrates for such applications.^{1–7} In the present work, we describe the synthesis and physical-chemical characterization of a complex cubic perovskite oxide $\text{Ba}_2\text{HoNbO}_6$ (BHNO) for its use as a substrate and fabrication of $\text{LaBaCaCu}_3\text{O}_{7-\delta}$ (LBCCO) superconducting films. Structural characteristics, quantitative elemental analysis and surface morphology of synthe-

§Corresponding author.

sized composites were investigated by means of X-ray diffraction (XRD), energy-dispersive X-ray (EDX) and scanning electron microscopy (SEM), respectively.

LBCCO is one of the important family of high temperature superconductors exhibiting superconductivity around 78 K.^{8,9} The structure of LBCCO is analogous to that of tetragonal $\text{YBa}_2\text{Cu}_3\text{O}_{7-\delta}$ compound.¹⁰ Compared with orthorhombic $\text{YBa}_2\text{Cu}_3\text{O}_{7-\delta}$ superconductors, LBCCO presents a simpler structure and there are no twins in this material.¹¹ Moreover, few oxygen vacancies¹² and spiral dislocation¹³ have been detected.

The chemical stability of BHNO with LBCCO was examined by X-ray diffractometry of BHNO/LBCCO composites. Back-scattered scanning electron microscopy was used to study the interface interaction between BHNO and LBCCO materials in the BHNO/LBCCO composites. The effect of BHNO addition on the superconductivity of LBCCO was investigated by measuring the magnetic susceptibility of BHNO/LBCCO composites in the temperature range 5–300 K. Our studies show that BHNO is chemically and physically compatible with LBCCO superconductors and it could be a potential substrate material for the fabrication of high temperature superconducting films. The results are reported and discussed in this paper.

2. Experimental Setup

BHNO was prepared by solid-state reaction process. A stoichiometric mixture of high purity (99.99%) chemical constituents Ho_2O_3 , BaCO_3 , Nb_2O_5 was mixed thoroughly, palletized and calcined at temperature of 1100°C for 40 h. The calcined material was reground, pressed as circular discs and sintered at 1200°C for 60 h. All the above processing was carried out in an ambient atmosphere. Single-phase LBCCO superconducting polycrystalline materials were prepared by the standard solid-state reaction process reported in literature.^{8–10}

For the study of the structural characteristics of the materials, X-ray diffraction spectra of the samples were recorded by a Siemens D5000 X-ray diffractometer, using $\text{CuK}\alpha$ radiation ($\lambda = 1.5406 \text{ \AA}$). Quantitative elemental analysis of BHNO was carried out by Energy dispersive X-ray (EDX) technique. EDX spectra of the samples were recorded using an X-ray OXFORD model PENTAFET detector with Be-window and 128 eV resolution. The accelerating voltage used was 20 kV, the beam current up to 350 pA and a count of 100 s. Surface morphology and microstructure of BHNO were studied by scanning electron microscopy (SEM) using secondary electrons. SEM micrographs of BHNO were recorded by using a Leico-Cambridge model stereoscan 440 electron microscope.

For the study of chemical and physical compatibility, we synthesized BHNO/LBCCO composites with 0 to 30 wt% of BHNO component in the composites. For the synthesis of composites, the component materials were mixed in desired wt% ratios and the mixture was palletized as circular discs at a pressure of 2 ton/cm². These pellets were heat treated at 950°C for 24 h in flowing oxygen

and cooled down slowly at a rate of $2^\circ\text{C}/\text{min}$ to room temperature for proper oxygenation. The chemical stability of BHNO with LBCCO was examined by X-ray diffractometry of the BHNO/LBCCO composites. Back-scattered electron micrographs of the BHNO/LBCCO composites were recorded to examine the interface interaction between BHNO and LBCCO materials. The effect of BHNO addition on the superconductivity of LBCCO superconductors was investigated by measuring the AC magnetization of the BHNO/LBCCO composites in the temperature range 5–300 K, by using a Quantum Design SQUID magnetometer.

3. Results and Discussion

The powder X-ray diffraction (XRD) spectrum of single phase BHNO is shown in Fig. 1. The XRD spectrum of BHNO is similar to that expected for $A_2BB'O_6$ -type ordered complex cubic perovskites, reported in JCPDS files. Based on d spacing and intensity ratios, we have indexed the XRD spectrum of BHNO as an ordered complex cubic perovskite oxide. The experimental lattice parameter of BHNO, calculated from the XRD data, is $a = 8.439 \text{ \AA}$.

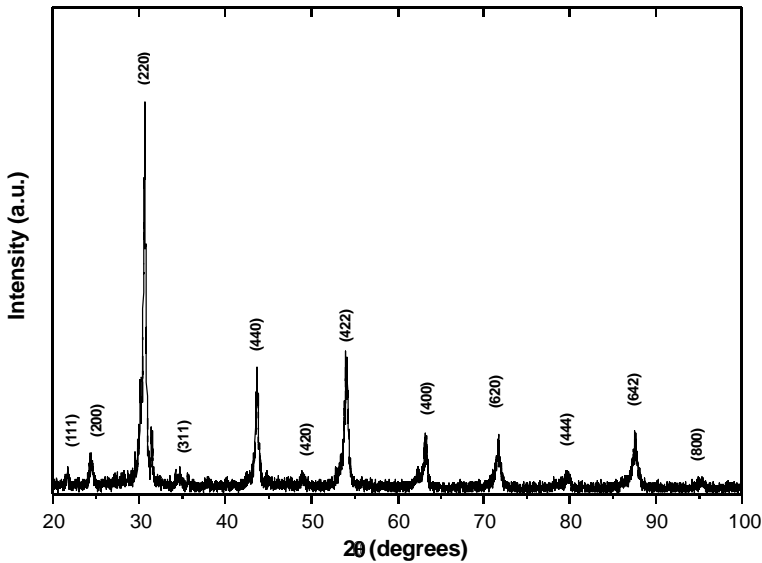


Fig. 1. X-ray diffraction spectrum of Ba_2HoNbO_6 .

Lattice matching of the superconductor with the substrate material is an important aspect for the fabrication of good quality superconducting films. In this context, it is worth pointing out that BHNO has a double cubic perovskite structure. Based on the doubling of the ABO_3 cubic perovskite unit cell, $(1/2)a = 4.220 \text{ \AA}$, BHNO has fairly good lattice matching with LBCCO (lattice parameters $a = 3.869 \text{ \AA}$ and $c = 11.617 \text{ \AA}$) superconductors. Calculated lattice mismatch between LBCCO and BHNO is $\sim 9\%$.

Table 1. Quantitative elemental analysis data of $\text{Ba}_2\text{HoNbO}_6$ obtained by EDX analysis.

Element	Element %	Atomic %
Ba	39.53	16.08
Ho	21.61	7.32
Nb	20.42	12.29
O	18.42	64.31
Total	100.00	100.00

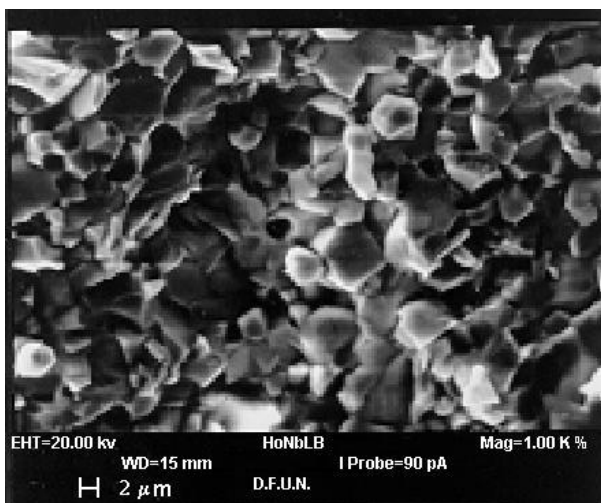


Fig. 2. Secondary electron SEM micrograph of sintered $\text{Ba}_2\text{HoNbO}_6$.

Energy-dispersive X-ray (EDX) analysis was performed on the sintered BHNO samples for the quantitative chemical analysis. The results of the EDX analysis are presented in Table 1. These results show that there is no evidence of any impurity traces in the single-phase BHNO materials. A secondary electron SEM micrograph of the sintered BHNO is shown in Fig. 2. The SEM micrograph shows that the surface of the BHNO sample presents the crystallinity of a typical polycrystalline ceramic material. As seen from Fig. 2, BHNO presents homogenous surface morphology and particle size distribution with average particle size 3–5 μm .

Chemical compatibility of BHNO with LBCCO superconductors was investigated by X-ray diffractometry of BHNO/LBCCO composite heat-treated at 900°C for 24 h. Figure 3 shows the X-ray diffraction (XRD) spectra of the BHNO/LBCCO composites. As seen from Fig. 3, all the XRD peaks correspond either to BHNO or LBCCO and there is no extra peak corresponding to any impurity phase. Within the accuracy of the X-ray diffraction technique, these results show that there is no

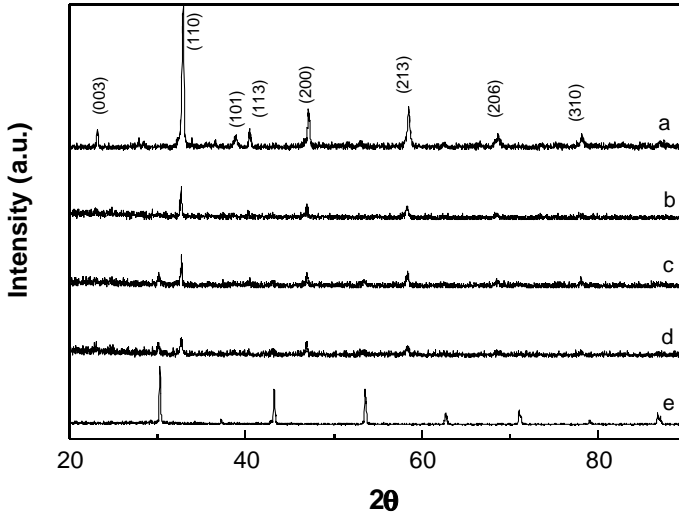


Fig. 3. XRD spectra of the Ba_2HoNbO_6 -LBCCO composites containing (a) 0 wt%, (b) 5 wt%, (c) 20 wt%, (d) 30 wt%, and (e) 100 wt% of Ba_2HoNbO_6 component.

chemical interaction between these materials and BHNO is chemically compatible with LBCCO superconductors.

Back-scattered electron microscopy was used for the study of the interface interaction between BHNO and LBCCO grains. In the back-scattered SEM, high-energy incident electrons undergo Rutherford scattering from the surface atoms and re-emerge from the surface. The resulting image is in some way like the secondary electron image, but there are a number of important differences. First, the back-scattered electron comes from a greater depth in the sample, and because of the spreading of the electrons in the sample, they represent a larger area. Also, since the back-scattered electrons come from deeper in the sample they contain less information about the surface and more about the bulk material.¹⁴ In the present work, back scattered electron micrographs of the BHNO, LBCCO and BHNO/LBCCO composite materials were recorded using a quarter back-scattering detector. These back-scattered electron micrographs are presented in Fig. 4(a)–(c). As seen from these micrographs, there is no detectable interface interaction between BHNO and LBCCO grain interfaces, and BHNO grains are distinguishably distributed in the LBCCO matrix.

To study the effect of BHNO addition on the superconducting properties of the LBCCO superconductors, AC magnetization measurements were carried out on the BHNO/LBCCO composites in the temperature range 5–300 K. Figure 5 shows the temperature dependence of the real part of the AC magnetization for BHNO/LBCCO composites. As seen from these figures, all the BHNO/LBCCO composites gave a superconducting transition temperature of 78 K as that of the pure LBCCO superconductor. A saturated diamagnetic transition is clearly

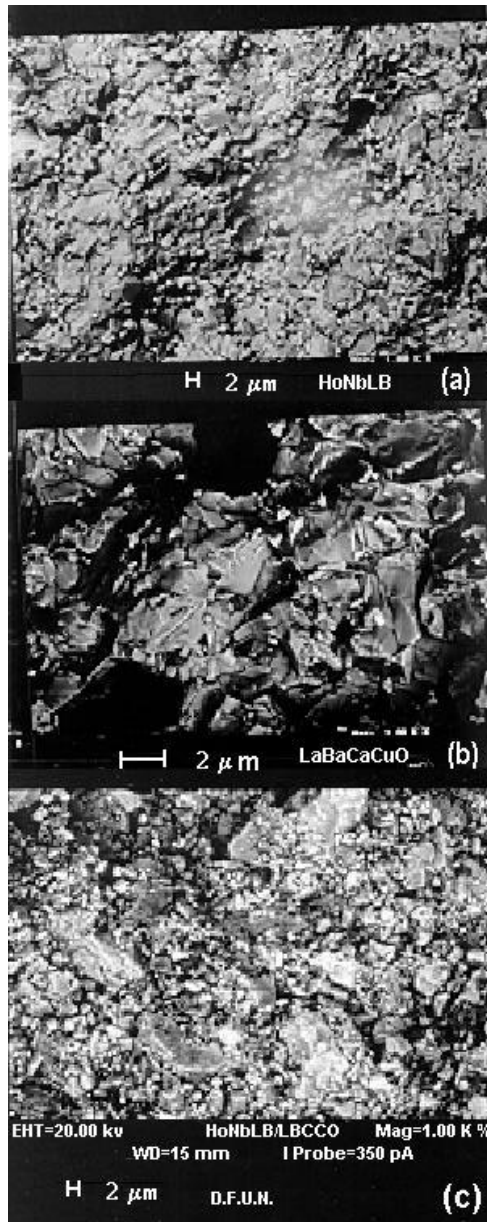


Fig. 4. Back-scattered SEM micrographs of (a) $\text{Ba}_2\text{HoNbO}_6$, (b) LBCCO, and (c) BHNO/LBCCO composite containing 30 wt% of $\text{Ba}_2\text{HoNbO}_6$ component.

observed in every sample at temperatures well below the critical temperature T_c . However, with decreasing LBCCO superconductor volume fraction, the magnitude of magnetization decreases in all the BHNO/LBCCO composite samples. It may be noted that the decrease in magnetization magnitude is more significant in com-

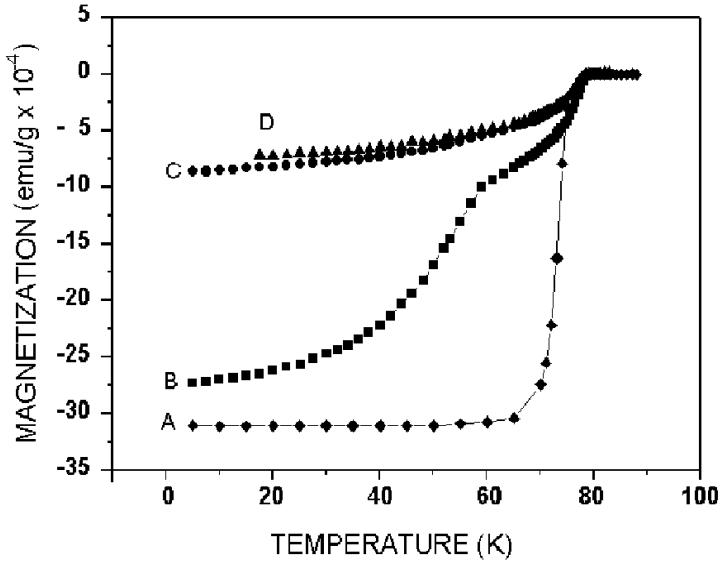


Fig. 5. AC magnetization as a function of temperature curves of BHNO/LBCCO composites containing (a) 0 wt%, (b) 5 wt%, (c) 20 wt%, and (d) 30 wt% of Ba_2HoNbO_6 component.

posites having higher wt% (> 20) of the BHNO component. This effect is most probably due to the percolation behavior of BHNO and LBCCO components in the composites. In a superconductor-insulator composite, the normal state and superconducting percolation threshold lie at ~ 17 vol%,¹⁵ as in the case of the metal-insulator composite.¹⁶ As we have observed and discussed earlier, the XRD studies show that BHNO and LBCCO are chemically non-reactive and remain as two distinct separate identities in the BHNO/LBCCO composites. Due to this percolating behavior, the decrease in magnetization in BHNO/LBCCO composites with the BHNO component up to 20 wt% is less significant than those having higher volume fraction of the BHNO component.

Furthermore, the presence of the second magnetization step below ~ 70 K in BHNO/LBCCO composites having 5 wt% of BHNO component as observed in Fig. 5(b). It has an intergranular origin and is due to the proximity effect and Josephson coupling between weakly coupled LBCCO grains.^{17,18} A similar phenomenon has been observed and detailed in the case of MgO/LBCCO composites.¹⁹ This step in the magnetization curve is not due to, say, a second superconducting phase with a lower T_c or due to oxygen deficiency. All the BHNO/LBCCO composites were heat treated at 950°C for 24 h in flowing oxygen and cooled down slowly at a rate of $2^\circ\text{C}/\text{min}$ to room temperature for proper oxygenation.

These results show that there is no deteriorating effect on the superconducting properties of the LBCCO superconductors due to the addition of BHNO, an insulating material, even up to 30 wt% addition and severe heat treatment at 950°C for 24 h and BHNO is physically compatible with these superconductors.

4. Conclusion

In conclusion, we have successfully synthesized a complex cubic perovskite oxide BHNO and studied its characteristics as substrate for the fabrication of LBCCO superconducting films. BHNO has fairly good lattice matching (lattice mismatch $\sim 9\text{--}10\%$) with these superconductors. X-ray diffractometry, back-scattered scanning electron microscopy and magnetic measurements effectuated on BHNO/LBCCO composites show that BHNO is chemically and physically compatible with LBCCO and it could be used as a potential substrate material for the fabrication of LBCCO superconducting films.

Acknowledgments

Brazilian Research Agencies CNPq, CAPES, FACEPE and FINEP financed this work. Y. P. Yadava would like to acknowledge CAPES. D. A. Landínez Téllez and J. Roa-Rojas would like to acknowledge CNPq and the Colombian Science Agency, COLCIENCIAS.

References

1. C. D. Brandle and V. J. Fratello, *J. Mater. Res.* **5**, 2160 (1990).
2. J. Koshy, J. Kurian, J. K. Thomas, Y. P. Yadava and A. D. Damodaran, *Jpn. J. Appl. Phys.* **38**, 117 (1994).
3. W. T. Fu and D. J. W. Ijdo, *J. Solid. State Chem.* **128**, 323 (1997).
4. J. A. Alonso, C. Cascales, P. Garcia Casado and I. Rasines, *J. Solid State Chem.* **128**, 247 (1997).
5. Y. P. Yadava, D. A. L. Téllez, M. T. de Melo, J. M. Ferreira and J. Albino Aguiar, *Appl. Phys.* **A66**, 455 (1998).
6. J. Albino Aguiar, D. A. L. Téllez, Y. P. Yadava and J. M. Ferreira, *Phys. Rev.* **B58**, 2454 (1998).
7. J. Albino Aguiar, C. C. de Souza, Y. P. Yadava, D. A. L. Téllez and J. M. Ferreira, *Physica* **C307**, 189 (1998).
8. W. T. Fu, H. W. Zandbergen, C. J. van Der Beek and L. J. de Jongh, *Physica* **C156**, 133 (1988).
9. R. Singh, R. Lal, U. C. Upreti, D. K. Suri, A. V. Narlikar, V. P. S. Awana, J. Albino Aguiar and M. Shahabuddin, *Phys. Rev.* **B55**, 1216 (1997) and references therein.
10. J. L. Peung, P. Klavins, R. N. Shelton, H. B. Radousky, P. A. Hahn, L. Bernardez and M. Costantino, *Phys. Rev.* **B39**, 9074 (1989).
11. D. M. de Leeuw, C. A. H. Mutsaers, H. A. M. van Hal, H. Verweu, A. Harim and H. C. A. Smoorenburg, *Physica* **C156**, 126 (1988).
12. X. J. Zhang, J. S. Wang, Z. A. Xu, Z. K. Jiao and Q. R. Zhang, *Physica* **C232**, 277 (1994).
13. R. V. Rao, *J. Mater. Sci. Lett.* **11**, 145 (1992).
14. J. C. Russ in *Systematic Materials Analysis*, Vol. 6, eds. H. Richardson and R. V. Peterson (Academic Press, London, 1974).
15. J. Koshy, K. S. Kumar, J. Kurian, Y. P. Yadava and A. D. Damodaran, *Phys. Rev.* **B51**, 9096 (1995).
16. D. Stauffer, *Phys. Rep.* **54**, 1 (1979).

17. W. Widder, L. Bauerfeind, H. F. Braun, H. Burkherdt, D. Rainer, M. Bauer and H. Kinder, *Phys. Rev.* **B55**, 1254 (1997).
18. M. E. McHenry, M. P. Maley and J. O. Willis, *Phys. Rev.* **B40**, 1666 (1989).
19. D. A. L. Téllez, Y. P. Yadava, J. M. Ferreira and J. Albino Aguiar, *Supercond. Sci. Technol.* **12**, 39 (1999).